Winglet Effect on Induced Drag for a Cessna 172 Wing

Alexander Schumacher
Erik Sjögren
Tobias Persson

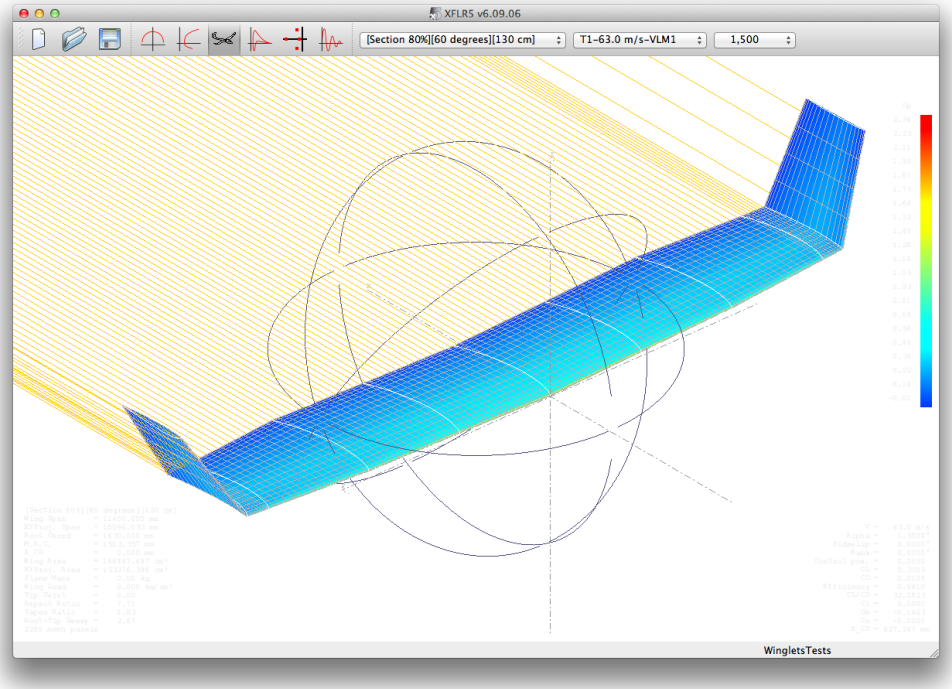

Bachelor Thesis 2014-05-18
KTH Flygteknik
Farkost och flyg
SE-100 44 STOCKHOLM

ABSTRACT

The perfect wing is a dream that many airplane manufactures have been striving to achieve since the beginning of the airplane. The goals are usually the same for everyone;

- Increase lift
- Reduce drag
- Minimize weight

A combination of these goals lead to a decrease in fuel consumption, which in turn reduces pollution in our atmosphere with the added bonus of an increase in economic revenue.

One way to improve performance is to modify the tip of the wing structure, which has become a common sight on today's airplanes. With the help of computational programs, the effects on drag due to wingtip devices can be previewed.

NOMENCLATURE

V	Free stream speed
α	Angle of attack
α_e	Effective angle of attack
α_i	Induced angle of attack
C_{Di}	Induced coefficient of drag
L	Lift force
ρ	Density
S	Wing reference area
e	Efficiency factor
AR	Aspect Ratio
b	Wingspan
c	Chord length
m	Mass
T	Thrust Force
g	Constant of gravity
D	Drag Force
C_L	Coefficient of Lift
D_i	Induced Drag Force
q	Dynamic pressure

TABLE OF CONTENTS

1 INTRODUCTION

1.1 Background

Winglets are widely used on larger commercial and military aircrafts to reduce fuel consumption by minimizing drag and maintaining or increasing lift. These winglets are usually not as common on smaller aircrafts that are found in general aviation. Here a question arose as to how much do winglets affect an aircraft, and what aeronautical effects result from these winglets? What happens to the induced drag caused by the winglets? Do the resulting structural loads on the wing vary drastically? Can these winglets be applied to the wings of a general aviation aircraft and will it be beneficial?

Since its start in 1955, more Cessna 172s have been built than any other aircraft [1]. The classic, almost rectangular, wing is easy to spot with it resting on the canopy of its body. The Cessna 172's popularity makes it a great candidate to use as a reference wing for winglet testing within general aviation.

XFLR5 is a well-used platform amongst hobby builders and airplane architects that want to experiment on new or old wing designs. The program is a tool that that lets users program wing designs and analysis based on the Lifting Line Theory, Vortex Lattice Method, and on 3-D Panel Method. Here a user can define a wing at a series of angles of attack, at different speeds, and with varying conditions. XFLR5 gives the user the opportunity to make their own wing and put it through thousands of tests. Everything from a 2-D airfoil to a 3-D CAD of the wing can be done in XFLR5.

In the following chapters the wing of a Cessna 172 will undergo several winglet modifications and be tested to see what effects they have on a wing. These modifications can be done thanks to XFLR5 with a goal to decrease the drag without creating too much structural load on the aircraft. Several key factors include the flight conditions, twist distribution, the design of the winglets, and the net forces resulting from the above modifications.

1.2 Purpose

With the help of XFLR5 a replica Cessna 172 wing will be modeled and wingtips will be applied to the existing wing to see what effects these cause on the aerodynamics of the wing. The wing lengths and wingtip designs will vary. A comparison of these winglets will help the reader gain an insight on winglets and their effects on the induced and total drags without increasing structural loads at a steady-state flight.

The following chapters will inform the reader about XFLR5, how to orientate oneself in the program, and how to retrieve data on a custom designed wing. XFLR5 reduces the need to build a physical model of a wing or plane, making it a cheap and quick way to retrieve data that may be vital for a plane to fly effectively.

1.3 Delimitations

The contents of the report are strictly focused on the aerodynamics of the wing of a Cessna 172 and what effects modifications of the wing have on the resulting data. The physics of the airplane will not be discussed passed the point of a general discussion. The data that is generated will be used to look at the induced and total drags created by different winglets on a Cessna 172 wing at steady-state flight. The bending moment along the root of the wing will be discussed as well.

The program XFLR5 will be used to the extent that only a main wing will be analyzed instead of the whole body of a plane or rear tail wing. The defining analysis will be constructed with a varying angle of attack and a constant speed. Plane inertia is used along with the option of viscosity. Several airplane and flight conditions will remain constant throughout the project.

1.4 Method

There are many factors that need to be taken into consideration in order to analyze the aeronautical effects that wingtips have on a set wing. With the decision to use a Cessna 172 wing it is essential that the original wing can be designed and programmed in XFLR5. A detailed description of the main structures of a Cessna 172 wing can be found in *Jane's All the World's Aircraft* [2]. Some key features include a NACA 2412 airfoil, root and tip chords, dihedral angles, and incidence angles. These features are later implemented in XFLR5 to build the wing. Once the wing is built, tests can be run at a constant velocity and varying angles of attack to see how the wing behaves in flight. The vortex lattice method is applied across the wing to help compute lift and induced drag at different parts of the wing. These results are used as a reference to compare the effects of adding wingtips to the original wing.

To understand the properties of winglets on a wing, one form of winglet is chosen. There are several variables that can be changed on this winglet design. The dihedral angle of the winglet, the length of the wing/winglet, and the twist distribution along the wing are a few key factors of the winglet design. Most of these factors will be tested and compared against each other and ultimately compared to the original Cessna 172 wing that is used today.

In order to compare the results of every new wing, the induced drag and total drag are exported from XFLR5 to MATLAB. The exported values are later interpolated and/or plotted so that graphs can be set up to help analyze the data.

2 THEORY

2.1 Wingtip Design

Wingtip designs have been debated and discussed since the early 20th century. There are nearly an infinite amount of varying styles for winglets and other wingtip devices that have previously been tested; some of these can be seen in Figure 2.1:

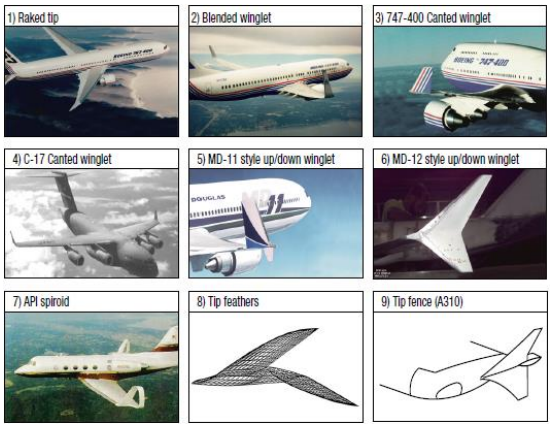

Figure 2.1. Different wingtip styles [3]

The true benefits of winglets have yet to be fully understood. There are many misconceptions about how a winglet works, and what it actually does. Winglets are used to reduce trailing vortex turbulence behind the wing, customize the lift distribution along the wing, and to increase the aspect ratio without having to increase the wingspan. The former being the idea that winglets can reduce the amount of induced drag from the wings. This is hard to achieve without increasing weight, or profile drag due to an increase in wetted area and junction flows. There are a few common misunderstandings about winglets that are important to discuss. The two most common misconceptions can be read in D. McLean's paper: *Wingtip Devices: What They Do and How They Do It* [3]:

- The "compactness myth"- the idea that the cores that contain all of the vorticity in the vortex wake after rollup are very compact.
- The "induction myth"- the trailing vortex sheet and the rolled-up vortex cores are the direct cause of the vorticities everywhere else in the flow field and of induced drag.

The combination of the two points above gives an idea that induced drag is caused by the vortex wake and that by making a local change to the flow in the core of a "tip vortex" will have a large effect on the induced drag. This is extremely misleading.

Even with the help of mathematical theories, it is hard to design a bettered winglet. There are no easy equations that give a detailed view of how the drag is affected by the varying modifications of the winglets or the lift distribution. Although, the Trefftz-plane theory does explain that a vertical winglet is most effective at reducing induced drag at the tip of the wing [3]. Through testing several different samples of winglets, Cone was able to decipher that "any non-planar shape that adds vertical height near the tip could reduce drag" [3].

Important to note is that a reduction in induced drag does not guarantee a net drag benefit. An increase in parasitic drag due to addition of wetted area and junction flows may negatively affect the total drag of the new wing. The attachment of wingtips will most likely increase the bending

moments on the entire wing resulting in a remodeling of the wing structure. This may cause a greater total weight for the airplane, which will affect the flying benefits negatively.

Another factor that helps the effectiveness of the wing with an attached winglet is the twist distribution. Attaching a winglet to an already optimized wing with a specific twist will most likely not contribute to the net benefit. This means that attaching a winglet to the wing may mean that a new twist distribution along the wing must be designed in order to optimize the new wing.

An important theme to keep in mind for winglet design is Whitcomb's rule of thumb; "keep the additional profile drag to a minimum through good aerodynamic design practice" [3], and "for a given increase in bending moment, a near-vertical winglet offers nearly twice as much drag reduction as a horizontal span extension." [3]. Important to note is that, many other studies such as, R.T. Jones' 1980 paper, show that with a fixed structural weight, the induced drag reduction is relatively the same.

2.2 Induced drag and minimum induced drag

2.2.1 Induced drag

The basic principle of generating lift on a wing is to achieve a lower pressure on the upper surface of the wing compared to the lower. Consequently, a global flow pattern is obtained which is shown in Figure 2.2.

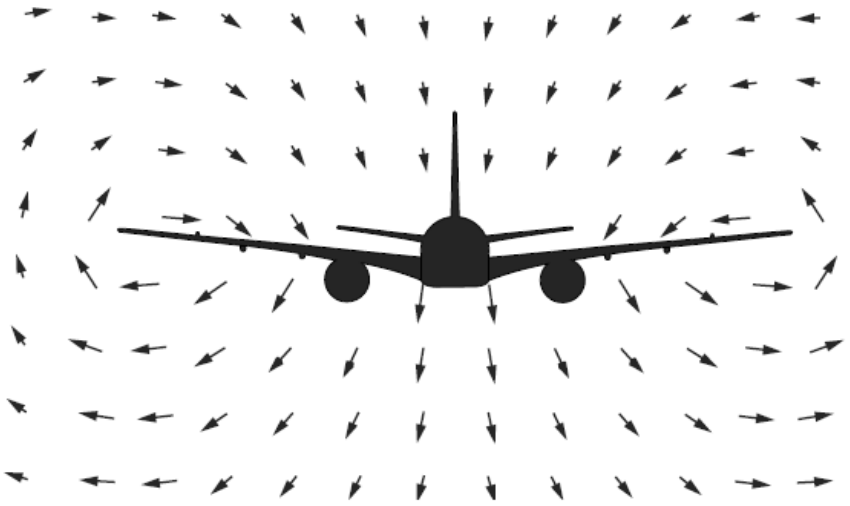

Figure 2.2. Global flow pattern [3]

When producing lift on a wing, the air from the underside of the wing will move outwards from the root and around the wing tip to meet the lower pressure flow. This reduces the pressure difference and is known as the span-wise pressure gradient. The effects of the pressure gradient decreases towards the wing root. As viewed from the front or rear of the aircraft the upward flow at the wingtips seems to produce vortices, also called trailing vortices. The vortices around the wing change the upstream airflow near the wing and deflects the flow down, also known as downwash. This leads to a decrease in the effective angle of attack due to the upstream flow near the wing being deflected down. The decrease in the effective angle of attack leads to a reduction in the lift force on the wing. Since all of the input energy for flight that does not contribute to the lift on the wing can be considered as drag, the loss of lift is felt as an extra drag, which is known as lift induced drag (a consequence of generated lift). An illustration of the induced drag is

shown in Figure 2.3, where V is the free stream direction, α is the angle of attack, α_e the effective angle of attack and α_i the induced angle of attack.

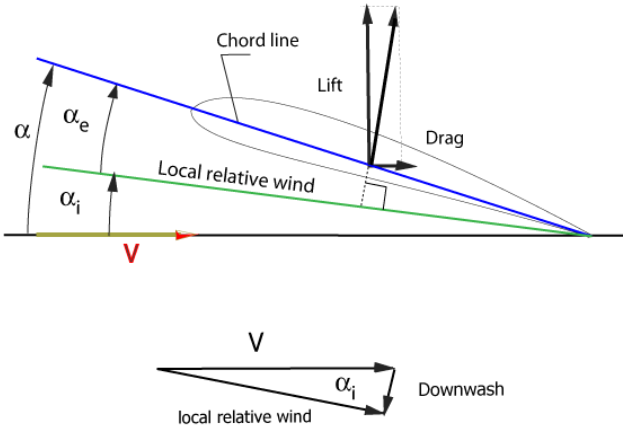

Figure 2.3. Illustration of induced drag.

The induced drag coefficient can be expressed as:

$$C_{Di} = \frac{L^2}{\frac{1}{4}\rho^2 V^4 S^2 \pi e AR}, \tag{2.1}$$

where L is the lift force, ρ is the free stream density, S is the wing reference area, e is the wing span efficiency factor by which the induced drag exceeds that of an elliptical distribution and AR is the aspect ratio. The aspect ratio is defined by

$$AR = \frac{b^2}{S}, \tag{2.2}$$

where b is the total wingspan. As one can observe, the induced drag is proportional to the lift force squared and inversely proportional to the aspect ratio.

2.2.2 Minimum induced drag

It can be shown that for a given wingspan and lift, minimum induced drag is produced when the span-wise lift distribution is elliptical [4]. This is valid for a planar wing. For a wing where the planar wing assumption is not accurate, the elliptic span-wise lift distribution may not be optimal.

2.3 Twist Distribution

By applying a lateral twist on a planar wing, one can begin to change the span-wise distribution of lift. By “twisting” the wing, the local angle of attack is changed resulting in a change on the local lift coefficients. On a “flat” wing, an elliptical distribution is optimum [4]. The difference in wing shapes lead to different wing twist distributions. It is important to note that in order to avoid stalling, the wing must be designed so that the stall begins as close to the wing root as possible [5]. A few examples of wing styles can be seen in Figure 2.4 below:

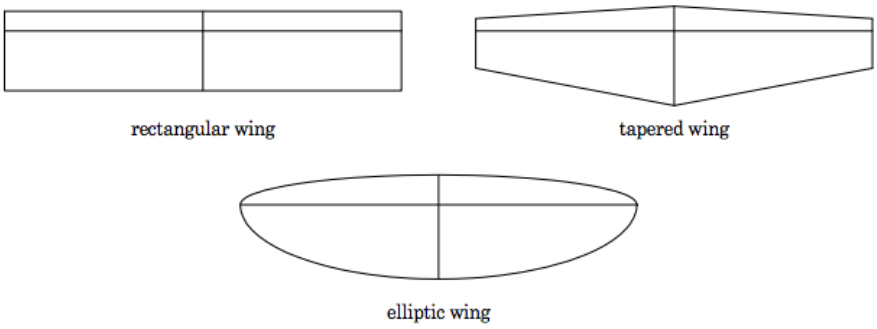

Figure 2.4. Three examples of planar wings [6]

From Arne Karlsson's notes on elliptic load distribution [5], a planar wing with an elliptic load distribution is represented from the following equation,

$$\left[\alpha_g - \alpha_i\right] c(\eta) = \frac{2}{\pi^2}\frac{C_L b}{AR}\sqrt{1-\eta^2}\,, \tag{2.3}$$

where

$$\alpha_i = \frac{C_L}{\pi AR}\,. \tag{2.4}$$

Here, α_g is the geometric angle of attack and α_i is the induced angle of attack. η is the dimensionless lateral coordinate along the wing, with 0 at the wing root, and 1 at the wing tip. *c* is the chord length and *b* the wing span.

For a thin section of the airfoil the local lift coefficient is used:

$$c_l = 2\pi\alpha_{eff}(\eta) = 2\pi\left[\alpha_g(\eta) - \alpha_i(\eta)\right]\,. \tag{2.5}$$

The effective angle of attack, α_{eff}, is measured from the zero-lift line of the airfoil section.

An elliptical wing, also known as a Spitfire wing, is already designed to have an elliptical distribution, meaning that there is no twist needed. For a rectangular wing with a constant chord, *c*, the twist distribution can be described by the following equation:

$$\alpha_g(\eta) = \alpha_i + \alpha_0\sqrt{1-\eta^2}\,, \tag{2.6}$$

where

$$\alpha_0 = \frac{2C_L}{\pi^2}\,. \tag{2.7}$$

The local lift coefficient at a lateral position along the wing is later found:

$$c_l(\eta) = 2\pi\alpha_0\sqrt{1-\eta^2}\,. \tag{2.8}$$

In the case of the Cessna 172, the wing is neither elliptical or rectangular. The wing is symmetric along the root chord, meaning that,

$$c_l(\eta) = c_l(-\eta). \tag{2.9}$$

From Equation (2.3) the lateral distribution of the geometric angle of attack is found:

$$\alpha_g(\eta) = \alpha_i + \frac{2}{\pi^2}\frac{C_L b}{ARc(\eta)}\sqrt{1-\eta^2}\ . \tag{2.10}$$

The span-wise distribution of c_l is found by combining the above equation with Equation (2.6):

$$\frac{c_l(\eta)}{C_L} = \frac{4}{\pi}\frac{b}{ARc(\eta)}\sqrt{1-\eta^2}\ . \tag{2.11}$$

The above equations are set towards finding an elliptic distribution along a planar wing, but when winglets are added the wing is no longer "flat." Here an elliptic distribution is not necessarily the most effective distribution for the wing. [3] These "ideal" distributions for a wing with winglets are different depending on how the wing will be used. The loads may be distributed depending on bending loads, and other factors such as engine position, fuselage, wing weight, etc.

2.4 Vortex lattice method

Analysis of a 3-D wing can be performed in XFLR5 using the Vortice Lattice Method (VLM). This method models the wing as a set of panels, all associated with a single horseshoe vortex. A horseshoe vortex consists of one vortex in the span-wise direction of the wing and two trailing vortices directed opposite the direction of flight, see Figure 2.4.

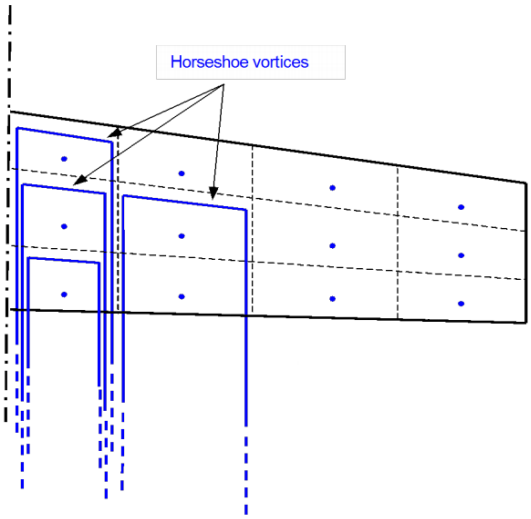

Figure 2.4. Horseshoe vortices defined for each panel of the wing [7]

As boundary conditions, the so-called no slip condition is used, which states that the velocity normal to the surface must be zero. The velocity on a panel depends on the free stream velocity but also on the velocity induced by the vortices on each of the panels. This gives a linear equation system from were the unknown vortex strengths can be solved.

When the circulation for each panel segment is known, the lift of a specific panel can be calculated with the Kutta-Joukowski theorem. Finally, the total lift of the wing is obtained by summating the lift contribution from all the panels.

In the classic vortex lattice method inviscid flow is considered. The XFLR5 implementation is however modified to take viscous effects into account. [7]

2.5 Steady Level Flight

Steady level flight is the point at which an aircraft is cruising at a constant speed. When flying at a constant speed, the airplane is in a state of inertia where all the acting forces on the airplane are in equilibrium. The general forces acting on the plane are seen in Figure 1 bellow,

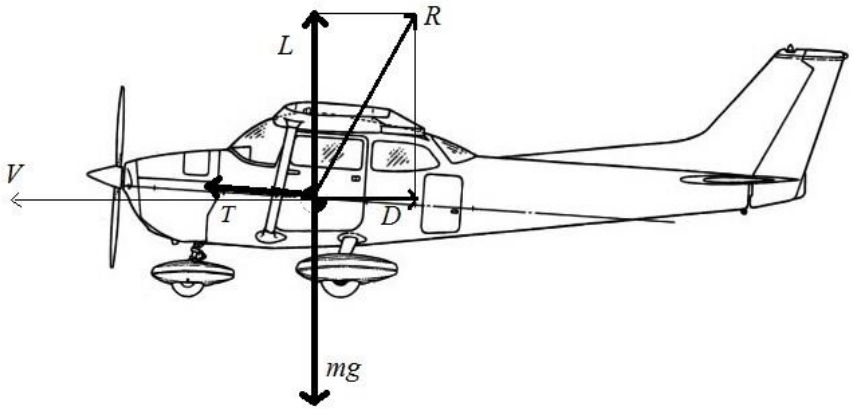

Figure 2.5. Free diagram of forces on a Cessna 172

Where *T* represents the thrust produced by the aerodynamic force *R*. The drag is defined as *D* in the figure above, as well as *L* represents the lift. In the free diagram, *mg* represents the force created by gravitational acceleration and the mass of the plane. The angle between the trust and velocity vectors is defined as ε. In a steady level flight there is no acceleration. As a result, all the forces must be balanced.

$$\uparrow: L + T\sin\varepsilon - mg = 0 \tag{2.12}$$

$$\rightarrow: L\cos\varepsilon - D = 0 \tag{2.13}$$

The angle between thrust and the speed vectors is usually small and for the following calculations $\varepsilon \approx 0$. From above, the following must be true:

$$L = mg\,, \tag{2.14}$$

and

$$T = D\,. \tag{2.15}$$

With the mass of the plane defined and the gravitational acceleration known, *L* can be defined. *L* is often assumed constant as long as *mg* does not change.

Important to note is the C_L that is calculated for the steady state flight does not exceed the maximum C_L where the wing will result in a stall. In order to find the C_L, the following equation can be used,

$$C_L = \frac{L}{\frac{1}{2}\rho V^2 S}\ , \qquad (2.16)$$

where ρ is the surrounding atmosphere density, V is the speed of the airplane, and S is the reference area of the wing. The calculated C_L for steady level flight must be less than the C_L at which the wing results in a stall. [8]

3 RESTRICTIONS

In order to compare the results from the modified wings, it is necessary to set up certain restrictions or definitions. These restrictions/definitions involve defining specific airplane designs, flight states, and winglet designs.

3.1 Airplane Modeling

To understand how the drag is affected along the varying wings, the body and tail wing of the Cessna 172 are ignored. The following procedures and results in this report are limited to strictly looking at the main wing. Here the values have been taken from *Jane's All the World's Aircraft* [3] for the original wing. For this project, it is inferred that all the lift on the airplane is done from this wing. Parts, such as the fuselage and wing flaps are not taken into consideration. Fluid effects from the propeller are also ignored.

Other airplane features that are disregarded are wing size, length, and weight. When looking to build a real wing, all three of these features should be analyzed. In this project, aspects such as typical garage heights and FAA limitations of wing lengths are not necessary when understanding the effects of wing designs on drag. Weight will have an impact on bending moments along the wing, as well as an increase in engine power or fuel consumption, although for this study effects on the plane due to weight are overlooked. The main focus is to look at how drag on the Cessna 172 wing changes due to different winglet designs, here the above three factors do not have a direct effect on the project.

The root bending moment constraint for all the wings in this project will be defined by the results for bending moment from the original twisted Cessna 172 wing in XFLR5. The root bending moments for the varying wings with winglets may not exceed this maximum by more than 0.5%.

3.2 Infinite Winglet Designs

There are an infinite amount of different winglet designs that can be applied to wings. Winglet size, twist, airfoil, design, and position are just a few parameters that need to be decided before beginning to compare effects on the induced drag. As for this study; the dihedral angles, winglet chords, winglet airfoils, and winglet positioning have been discussed and defined.

The resources and time allotted are not sufficient to consistently test the infinite different winglet configurations. The above restrictions, may not give the optimum winglet for the Cessna 172, but should be sufficient enough to see the effects that winglets do have on the wing.

3.3 Flight State

An airplane undergoes several flight positions once in flight. The behavior of the wing changes as the plane flies at different altitudes, speeds, climbs or descents, etc. In order to establish consistency, the plane is set at a steady level flight at a defined altitude with a constant speed and density. As seen in Equation (2.14), a desired lift force is defined and used. The winglets may affect the drag and lift differently at varying speeds or angles of attack, but as for this report the wing will strictly remain at a steady level flight.

4 METHOD

4.1 Analysis of a wing in XFLR5

4.1.1 Modeling of the Cessna wing

The following chapter describes how XFLR5 can be used for a wing analysis, more specifically, how an analysis can be performed on the wing of the Cessna 172. The program can produce a variety of data, including: the lift, drag, span-wise load distribution, and bending moment along the wing. Dimensions used to model the wing are taken from *Jane's All the World's Aircraft* [3] and can be seen in Table 4.1 below. The chord is defined as constant from the root to the middle section of the wing, this can be seen in Figure 4.1. Thereafter, the chord is linearly distributed to the tip. The used chord distribution is seen in Figure 4.2.

Cessna 172 Data	
Airfoil	NACA 2412
Wing Span	11 m
Root Chord	1.63 m
Tip Chord	1.13 m
Dihedral	1.7 °
Twist at root	1.5 °
Twist at tip	-1.5 °
AR (Aspect Ratio)	7.5

Table 4.1. Data for the Cessna 172 from Jane's All the World's Aircraft [3]

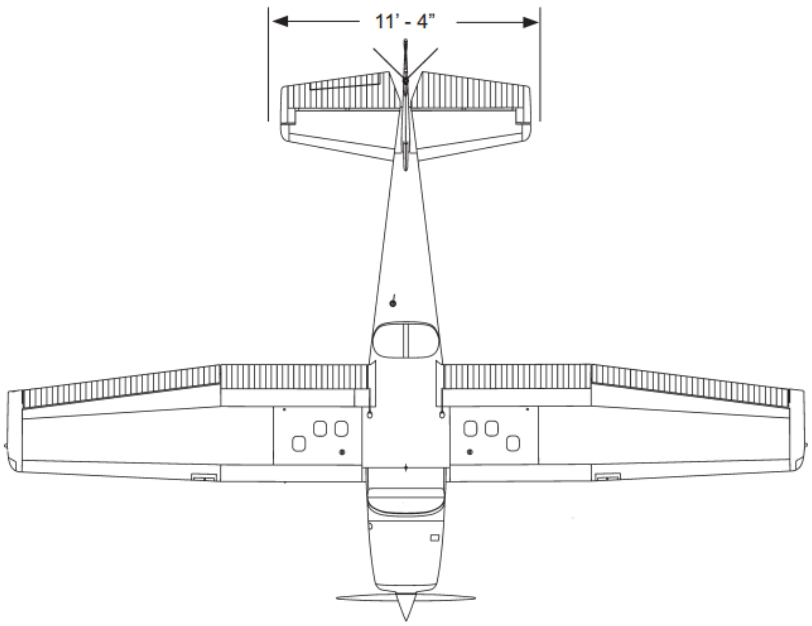

Figure 4.1. Top view of Cessna 172 [9]

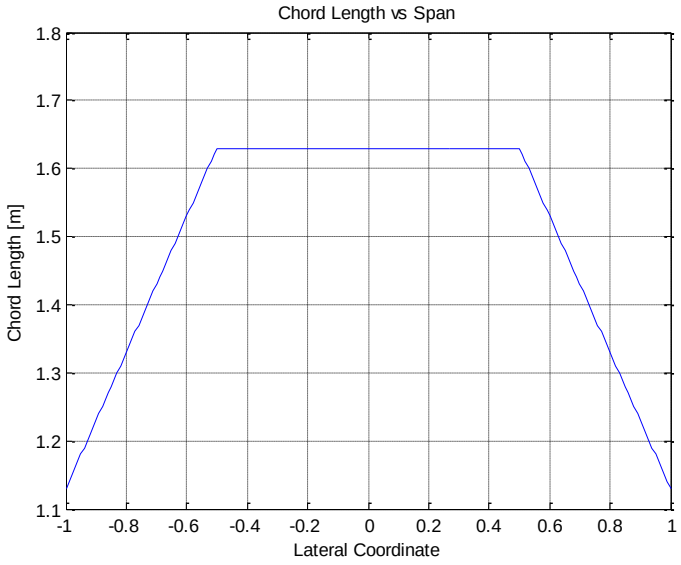

Figure 4.2. Estimated Distribution of Chord Length

In order to compare the different wings, the flight conditions must be specified. The chosen data representing a typical flight can be seen in Table 4.2 below. The values used for the speed and weight of the plane are taken from *Jane's All the World's Aircraft* [3]. The flying altitude is set to 2000 m. The remaining parameters are taken from the *US Standard Atmosphere* [10] and correspond to the chosen altitude.

Flight Data	
Cruising speed, Cessna 172R 80% power	63 m/s
Max T-O weight, Cessna 172R	1111 kg
Altitude	2000 m
Mach Number	0.19
Air Density	1.007 kg/m^3
Air Viscosity	$1.714 \cdot 10^{-5}$ m^2/s
Acceleration of Gravity	9.80 m^2/s

Table 4.2. Flight data used for the analysis

4.1.2 Airfoil analysis

The analysis of a wing in XFLR5 starts with the definition of an airfoil, which is done in the mode "Foil Direct Design". For this project the NACA 2412 airfoil of the Cessna wing is used. An analysis using a number of different conditions can be performed on the created airfoil. The analyzed data for a given condition is referred to as a polar and can be tested under the mode "Direct Foil Analysis".

In this project, a "Type 1" analysis is used for the polars, where the velocity is held constant and the flight data is calculated at different angles of attack. For the analysis, Reynolds number and the Mach number must be specified. The 3-D model of the wing is essentially built up from 2-D airfoils with varying chord lengths, meaning that the Reynolds number will vary along the span of the wing. Therefore, the range of Reynolds numbers used for the analysis should be decided according to the chord length of the wing. In a "Batch Foil Analysis" (Figure 3), the program allows the user to specify a range of Reynolds numbers where one can calculate the polars.

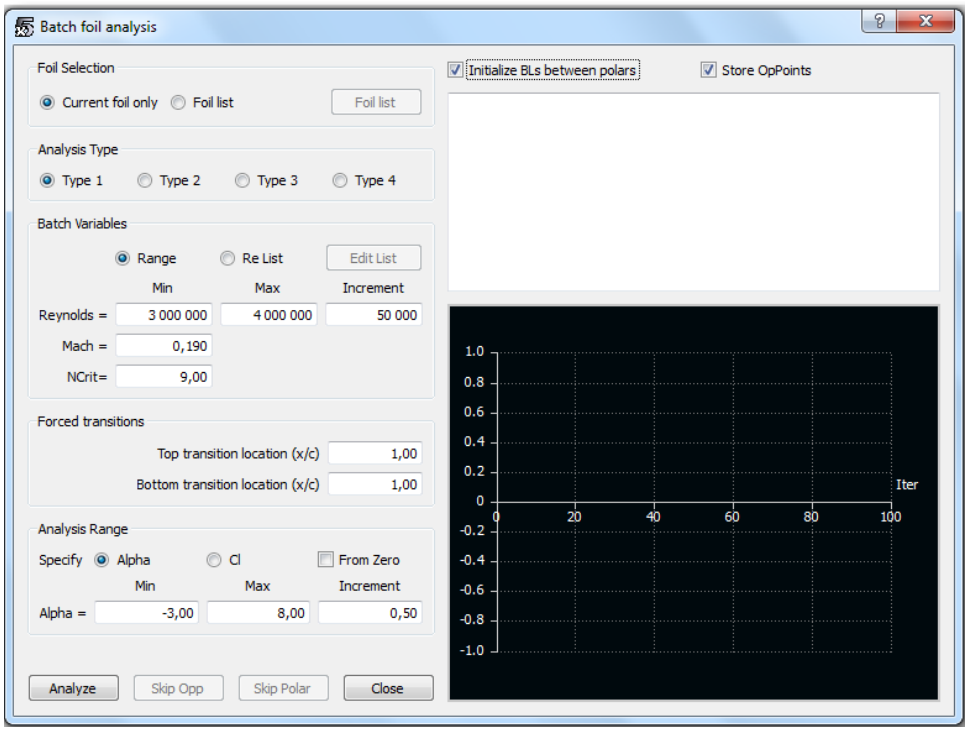

Fig 4.3. Analysis settings for a batch foil analysis in XFLR5

4.1.3 Wing analysis

With the generated polars, an analysis can be performed on the full 3-D wing in the "Wing and Plane Design" mode. The wing is created by defining cross sections at different span-wise positions along the wing. Each cross section is defined by its airfoil, chord length, dihedral angle, twist angle, and leading edge offset.

To create a specific twist distribution for the wing one must define the twist at a number of extra cross sections. In XFLR5, the twist distribution is linear between two cross sections. Extra cross sections are used as a form of discretization in order to achieve the preferred twist. This is done for the original Cessna 172 wing, where the desired twist distribution was decided from equation (2.10). For this report, it is assumed that an elliptic lift distribution is desired for the original wing. An important factor when twisting the wing is to make sure that the geometric angle of attack at the root is greater than the α_g at the wing tips in order to avoid stalling during flight.

The C_L corresponding to a steady level flight was used in equation (2.10). This C_L can be decided from equation (2.7) using L from equation (2.14). Figure 4.4 below shows how the different cross sections of the wing are defined.

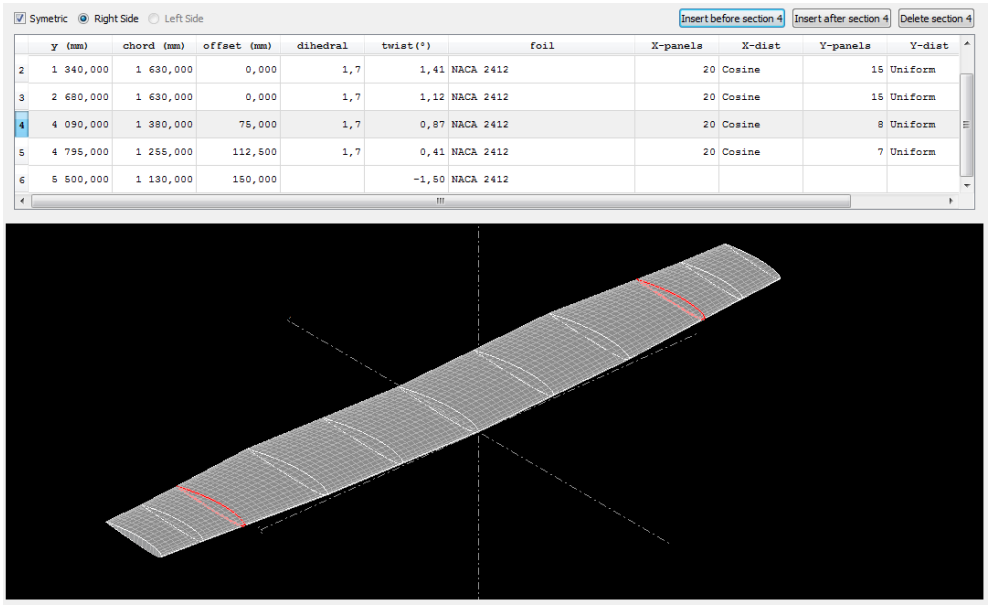

Figure 4.4: Defining a Wing With Different Cross Sections in XFLR5

XFLR5 offers different analysis methods, based on the lifting line theory (LLT), the vortex lattice method (VLM), and a 3-D panel method. For a wing with high dihedral angles, as in the case of winglets, the LLT is not recommended. The main use for the 3-D panel method is to take the effects of the plane's body into account. Since this project only focuses on the main wing, there is no need to use this method. Instead the VLM is used as it is most suitable for a wing with winglets.

Again, a "Type 1" analysis is performed in which the velocity is kept constant. Viscous effects are ignored in the classic VLM, however, XFLR5 offers an option to include viscous effects. These results are extrapolated from the 2-D model [11]. The viscous option is used in this project. Free stream speed, air density and viscosity from Table 4.2 are used, as seen in Figure 4.5.

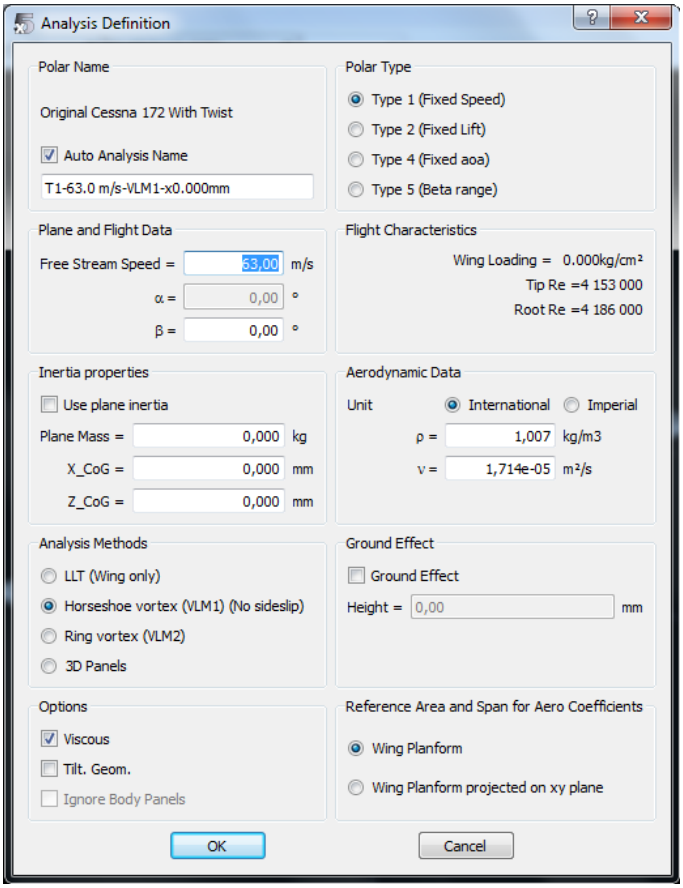

Figure 4.5. Settings for a wing analysis in XFLR5

4.1.4 Results from the analysis

After a completed analysis various data is returned to the user. In this project the lift, drag, and bending moment are studied and compared at each individual new wing design. The results can be studied in graphs directly in XFLR5, or exported to an Excel file, which is done in this project. The data is then read in MATLAB and analyzed in more detail.

4.2 Calculating and Comparing Winglets

4.2.1 Main Concept

In this chapter, an attempt to compare the effects from different winglets on the induced drag and total drag will be done. The flight state considered is the steady level flight, which has been discussed in Theory. From Equation (2.14), the lift force needed is equal to the weight of the plane (assumed to be constant for all winglets). The estimated mass of the plane and the gravitational acceleration can be seen in Table 4.2. The lift force needed is

$$L = mg = 1111 \cdot 9.80 \approx 10000 \ N. \qquad (4.1)$$

In order to have a thorough winglet comparison, as many parameters as possible are kept constant. The remaining parameters are systematically altered. As a start, the original wing is partitioned at 70 %, 80 % and 90 % of the total wingspan in the lateral direction. A visual graphic of this is seen in Figure 4.6.

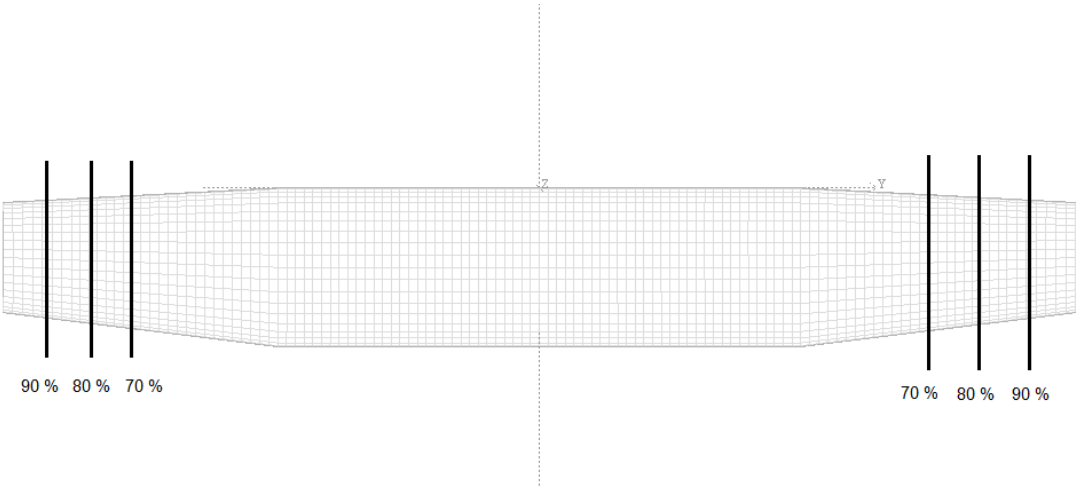

Figure 4.6. Sections of the original wing at 70 %, 80 % and 90 % of the wingspan

At each new section of the wing, wingtips of different lengths and dihedral angles are applied. The same junction, see Figure 4.7, is used for all of the winglets tested. This junction is obtained from a simple change in dihedral angle at the position where the winglet is applied. The airfoil is the same for all of the winglets and is the same NACA 2412 airfoil that is used for the original wing.

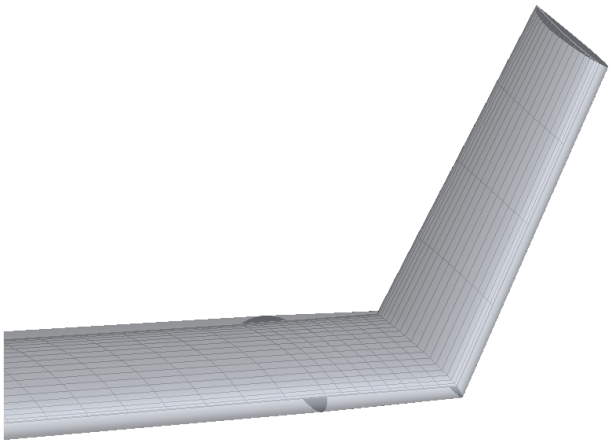

Figure 4.7. Junction of the winglets

Table 4.3 shows the systematic scheme of how the wingtips are designed.

Section	Dihedral angle	Wingtip length
70%	30	30
		80
		130
	60	30
		80
		130
	90	30
		80
		130
80%	30	30

		80
		130
	60	30
		80
		130
	90	30
		80
		130
90%	30	30
		80
		130
	60	30
		80
		130
	90	30
		80
		130

Table 4.3. Scheme of how variations of dihedral angles and wingtip lengths are made

4.2.2 Wing Data and Comparison

Without a moment constraint

A methodic overview of how to analyze the results from the varying winglets in Table 4.3 is presented here.

The relation between the global induced drag coefficient and the global lift coefficient at a discrete number of points is calculated with XFLR5. That is,

$$C_{D_i}[C_L], \tag{4.2}$$

where C_{Di} is the global induced drag coefficient. The induced drag coefficient can be defined as:

$$C_{Di} = \frac{D_i}{\frac{1}{2}\rho V^2 S}, \tag{4.3}$$

where D_i is the induced drag force.

The relation (4.2) can be modified to describe the forces related to the coefficients by multiplying the coefficients with the dynamic pressure q, which is defined as:

$$q = \frac{1}{2}\rho V^2 S \ . \tag{4.4}$$

From equation (2.16) and equation (4.3) one can see that this leads to the relation:

$$D_i[L], \tag{4.5}$$

where L is the lift force.

The discrete data points from XFLR5 are exported to MATLAB and interpolated to get the induced drag at the desired lift more accurately. A second order interpolation polynomial is used, as shown in Figure 6.

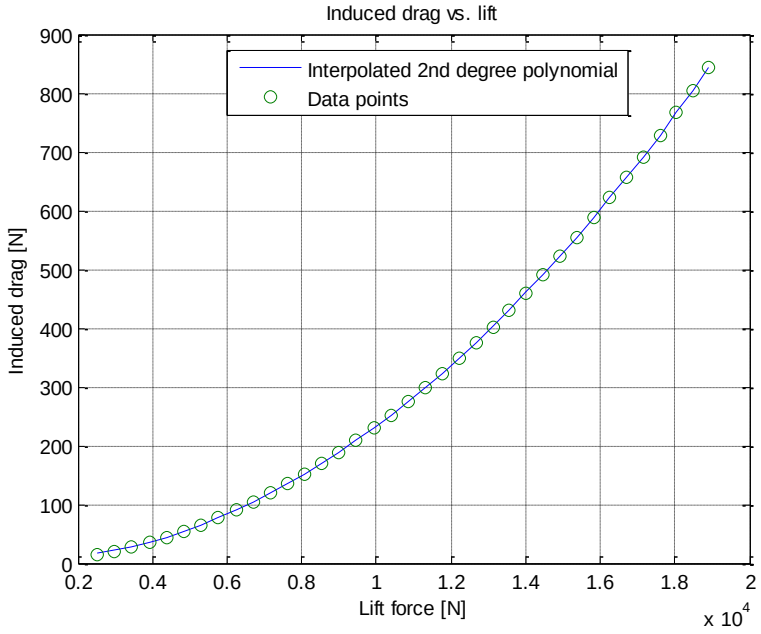

Figure 4.8 Interpolation of induced drag versus lift force

With a moment constraint

The winglet designs in Table 4.3 may not be optimal when trying to find the winglet effects at a given root bending moment constraint, instead, a new comparison is done. If one wishes to be able to compare different wings for a given airplane, in this case a Cessna 172, the root bending moment obtained from the wings with winglets applied should be the same as for the original wing. Some of the winglet configurations that follow from the scheme in Table 4.3 may exceed the root bending moment constraint. To achieve a better comparison, the scheme in Table 4.3 is modified so that for each dihedral angle, the wingtip length will be adjusted so the root bending moment will be equal to the original wing. To clarify this, Table 4.4 shows the new scheme followed here for one of the three sections.

Section	Dihedral angle [°]	Wingtip length [cm]
70 %	30	max
	60	max
	90	max

Table 4.4. Scheme of winglet designs to achieve the root bending moment constraint

Since the bending moment on a wing depends on the lift, it will vary with the angle of attack.
For each analyzed wing the angle of attack needed to maintain the steady level flight is calculated. This is done by looking at the linear relation between the lift force and the angle of attack. The data points calculated in XFLR5 are interpolated with a first degree polynomial as shown in Figure 4.9.

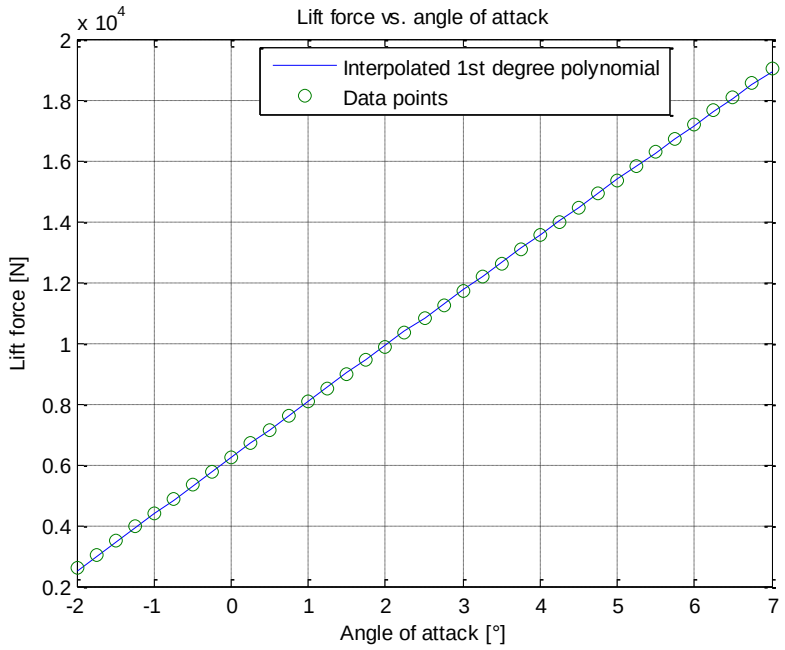

Figure 4.9 Interpolation of lift versus angle of attack

At the angle of attack that maintains the steady level flight, the bending moment distribution along the wing is obtained from data calculated by XFLR5, see Figure 4.10.

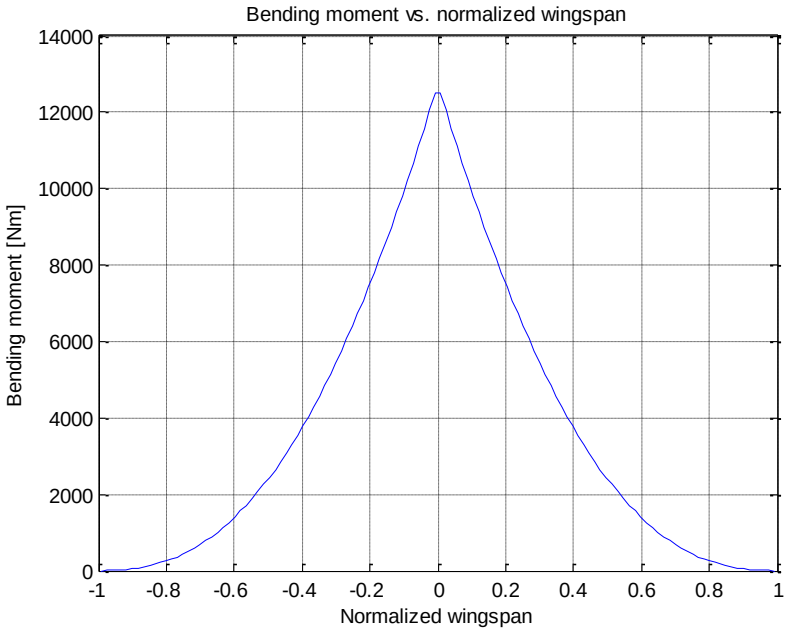

Figure 4.10. Typical wing bending moment curve.

The root bending moment is obtained from Figure 4.10 at the horizontal point 0. The moment distribution along the wing is related to a specific angle of attack and because the calculations in XFLR5 are made for a discrete number of angles of attacks, the root bending moment can only be obtained at these specified angles of attacks. To get a more accurate read of the root bending moment at the desired angle of attack, the root bending moment at different angle of attacks are interpolated with a first degree polynomial. An example of this is shown in Figure 4.11.

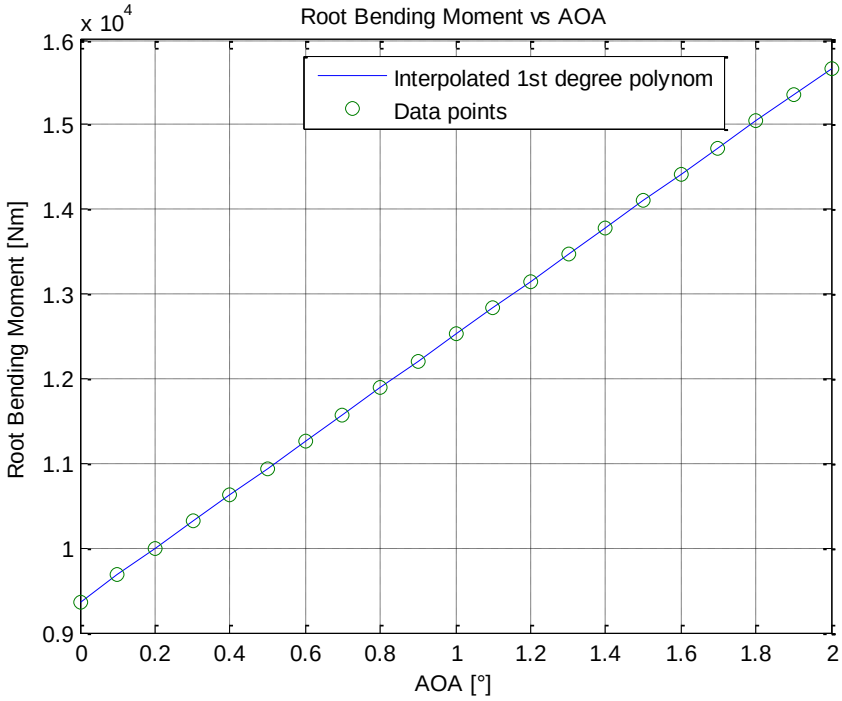

Figure 4.11. Interpolated root bending moment vs angle of attack

With the polynomial used in Figure 4.11, the root bending moment at the desired angle of attack where steady level flight is maintained can be calculated. The winglet sizes are adjusted so that the root bending moment is within a 0,5 % interval of the original wing. To achieve the root bending moment constraint at the desired lift for every winglet design, one needs to repeat the above steps to calculate the correct winglet length that gives the set root bending moment. As described in the previous section, the induced drag at the desired lift is calculated from a second order polynomial interpolation of the induced drag dependent on lift.

5 RESULTS

With the help of XFLR5 and MATLAB as mentioned in the above Method, the results from the tested winglets are easily compared. There are many ways to visualize the results in XFLR5; pressure, lift, induced drag, and panel forces are just a few of the many visual graphics that XFLR5 offers. The bellow pictures show just a few ways the results can be viewed:

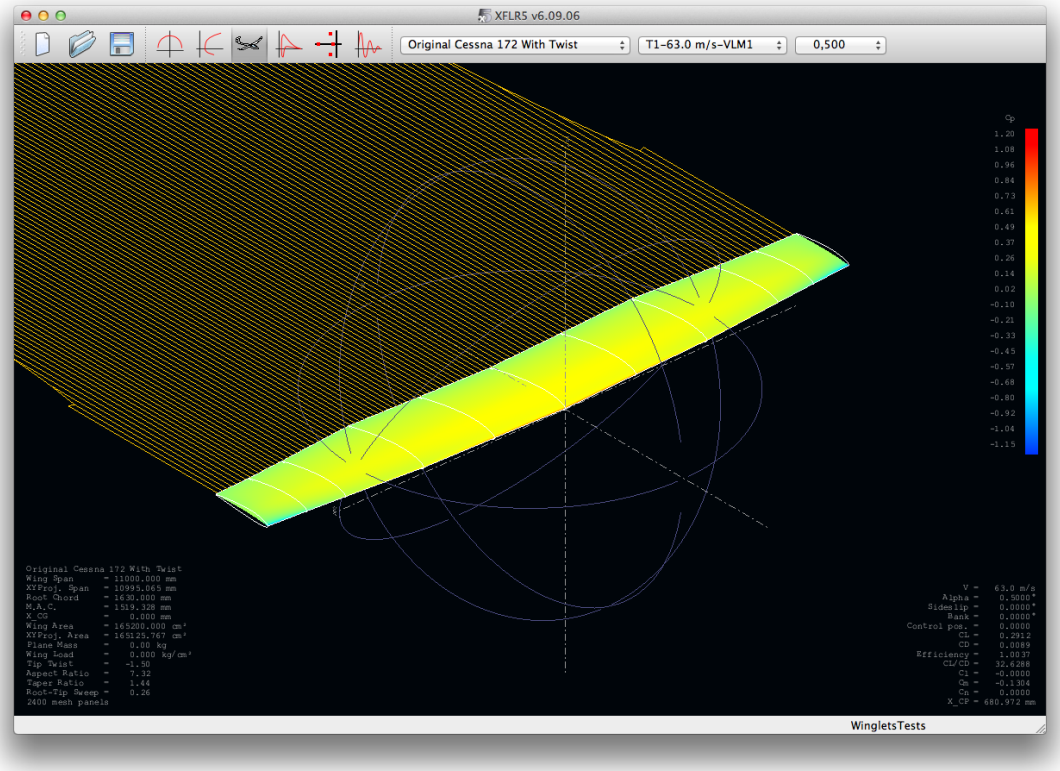

Figure 5.1. Graphic visual of pressure, C_p, and induced drag on the twisted Cessna 172 wing.

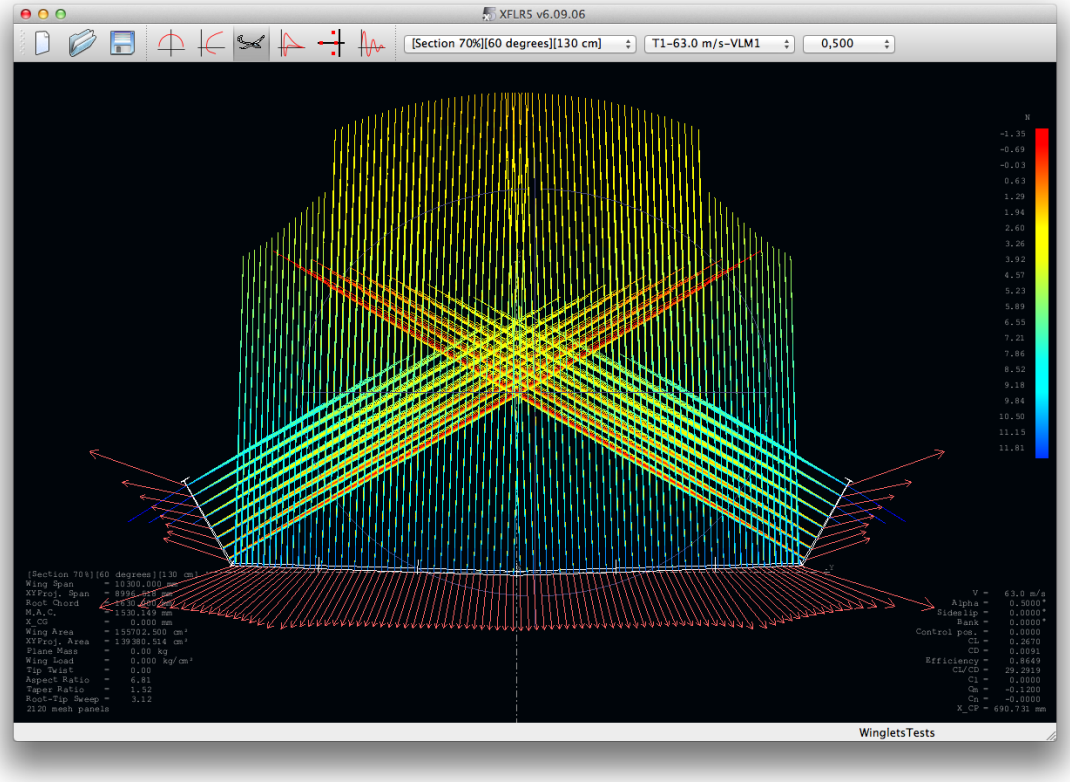

Figure 5.2. Graphic visual of the panel forces and downwash on 70% Cessna wing with 130cm winglets at 60°

In order to compare all of the results, the calculated values of each test are exported to MATLAB, where they are more closely analyzed. All of the winglet modifications are compared to the original Cessna 172 wing with and without an applied twist. The resulting graphs showing how induced drag is affected by varying winglets can be seen bellow:

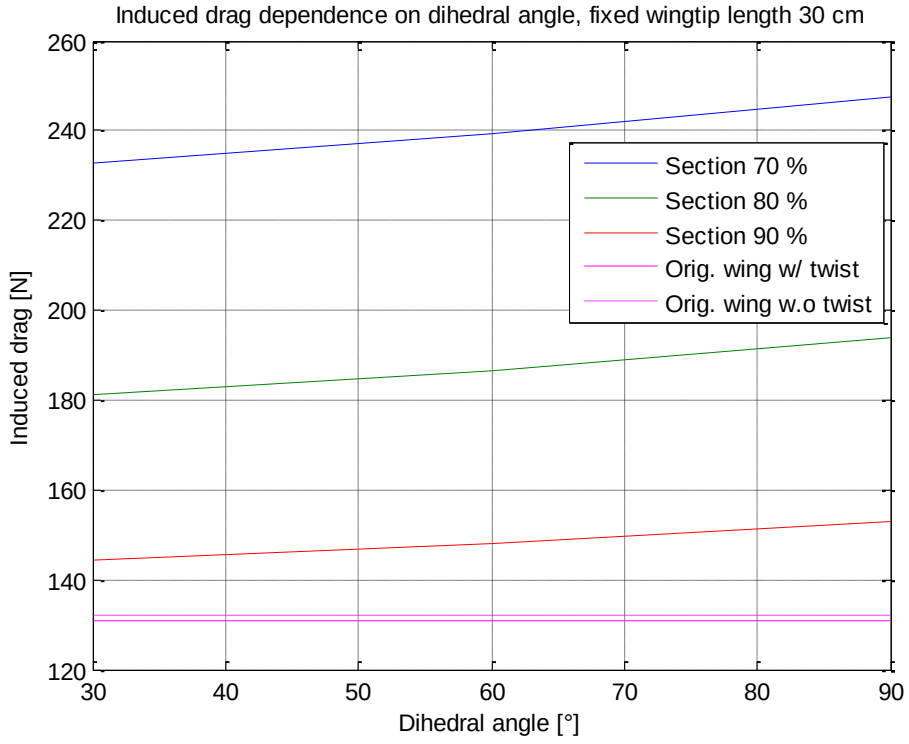

Figure 5.3. Induced drag with fixed wingtip length 30cm

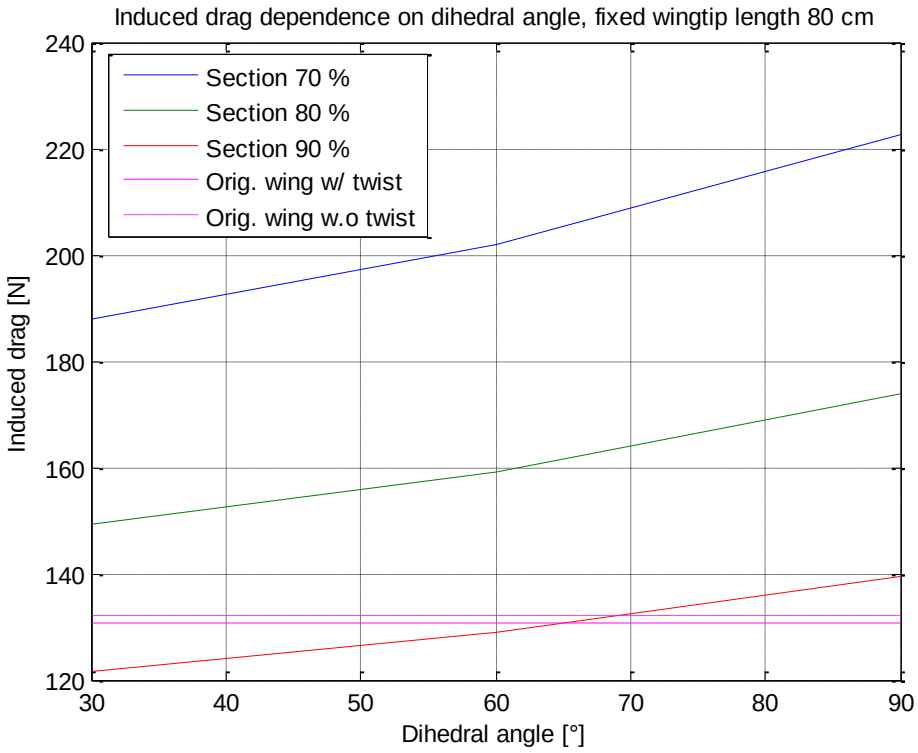

Figure 5.4: Induced drag with fixed wingtip length 80cm

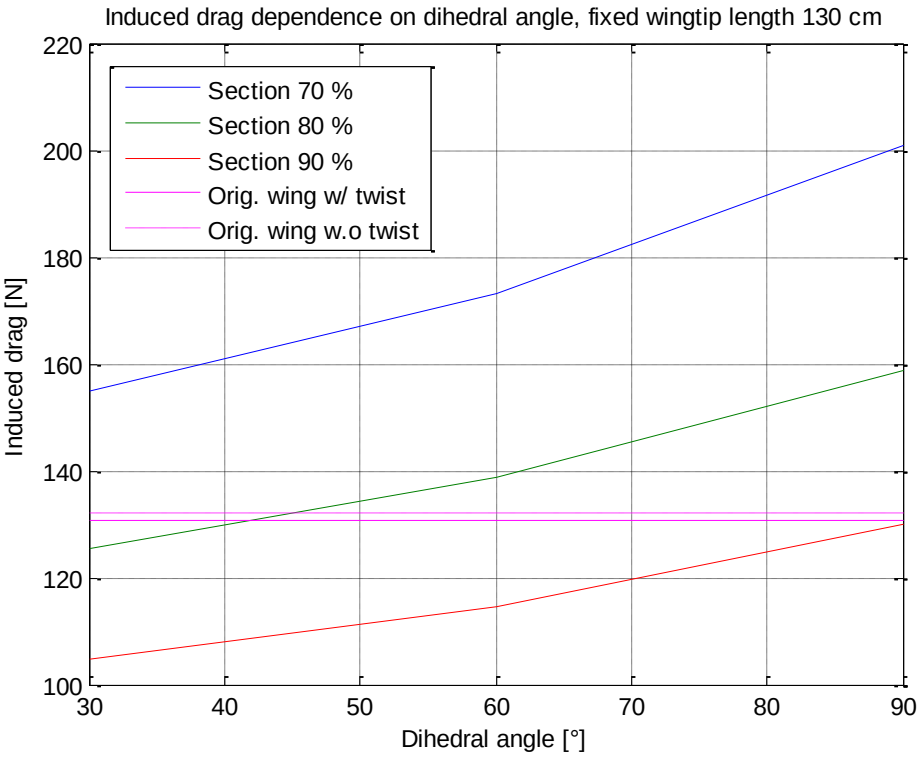

Figure 5.5. Induced drag with fixed wingtip length 130cm

After testing the three lengths of winglets at different positions along the wing and with varying dihedrals, one more set of tests are done on the wing. Here the lengths of the winglets are modified so that the root bending moment constraint is fulfilled at each wing position and dihedral. The following graph shows the resulting induced drag:

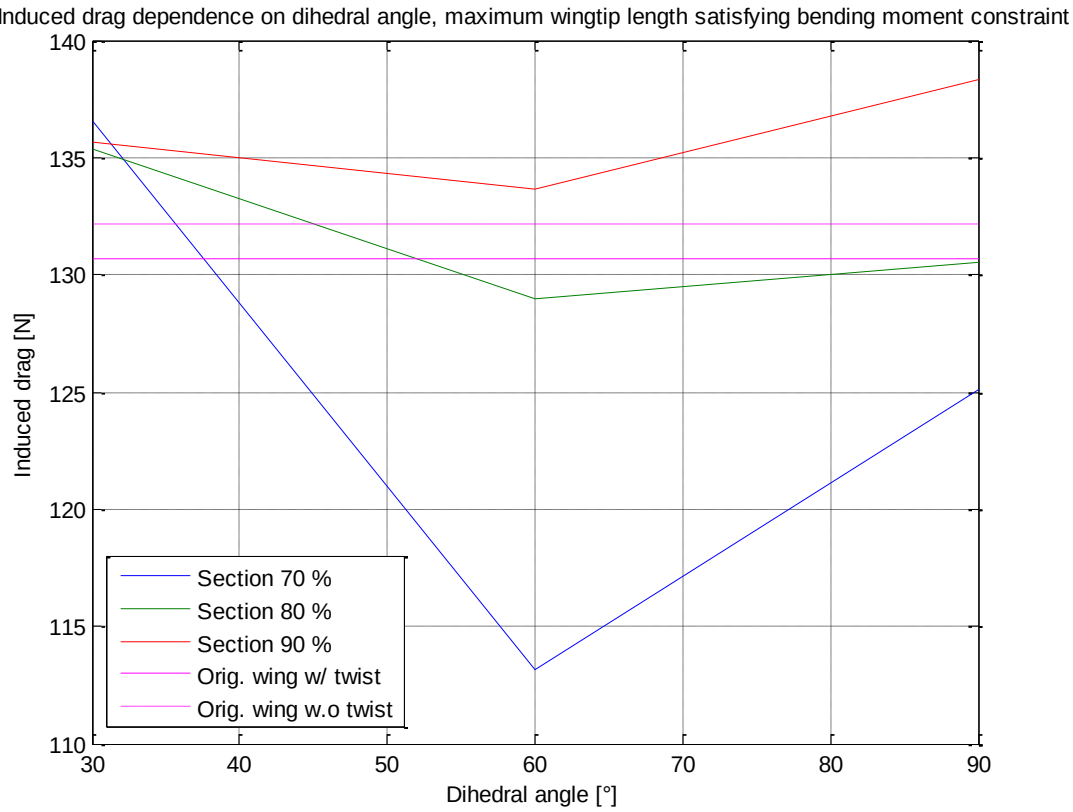

Figure 5.6. Induced drag with varying length limited to max. bending moment

After the induced drag is analyzed, it is a good idea to look at the total drag that results from the same winglet tests. From the above theory, a decrease in induced drag does not automatically account for a decrease in the total drag. The following graphs show how the total drag is affected by the same varying winglet modifications:

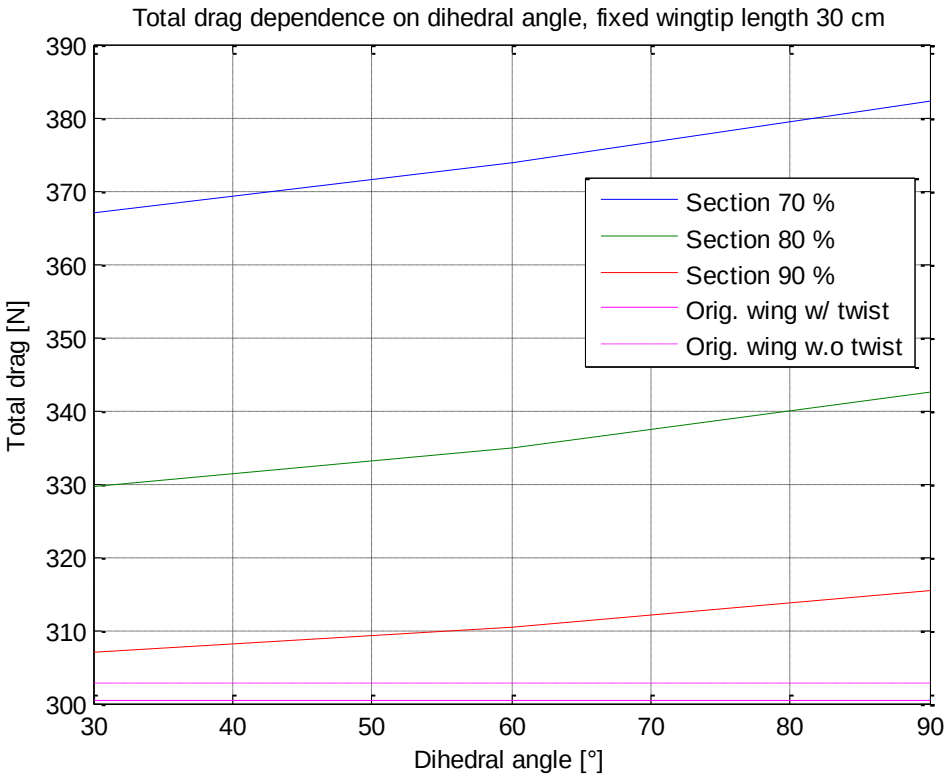

Figure 5.7. Total drag with fixed wingtip length 30cm

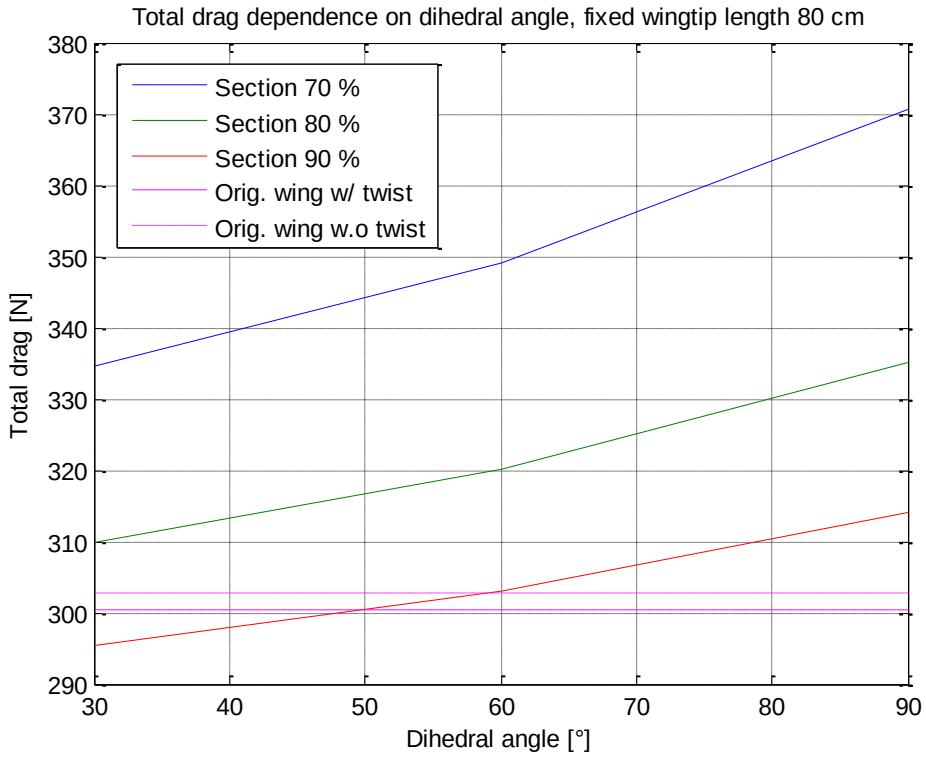

Figure 5.8. Total drag with fixed wingtip length 80cm

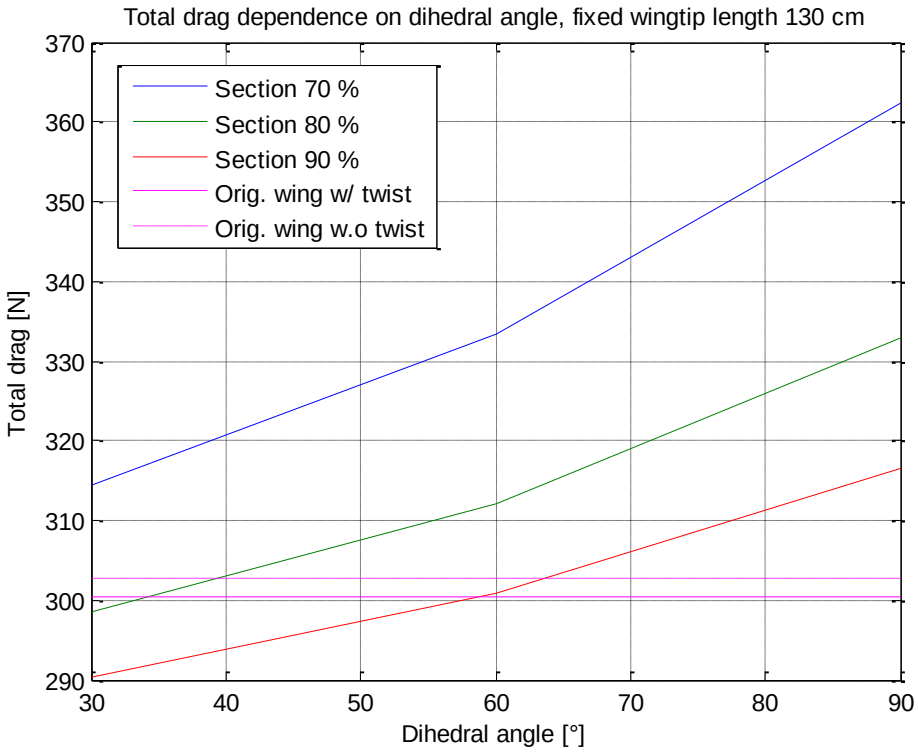

Figure 5.9. Total drag with fixed wingtip length 130cm

Just as the above tests, the lengths of the winglets were modified so that the root bending moment constraint was fulfilled at each wing position and dihedral. In the graph bellow, Figure 5.10, the total drag can be seen for the same winglet modifications as in Figure 5.6:

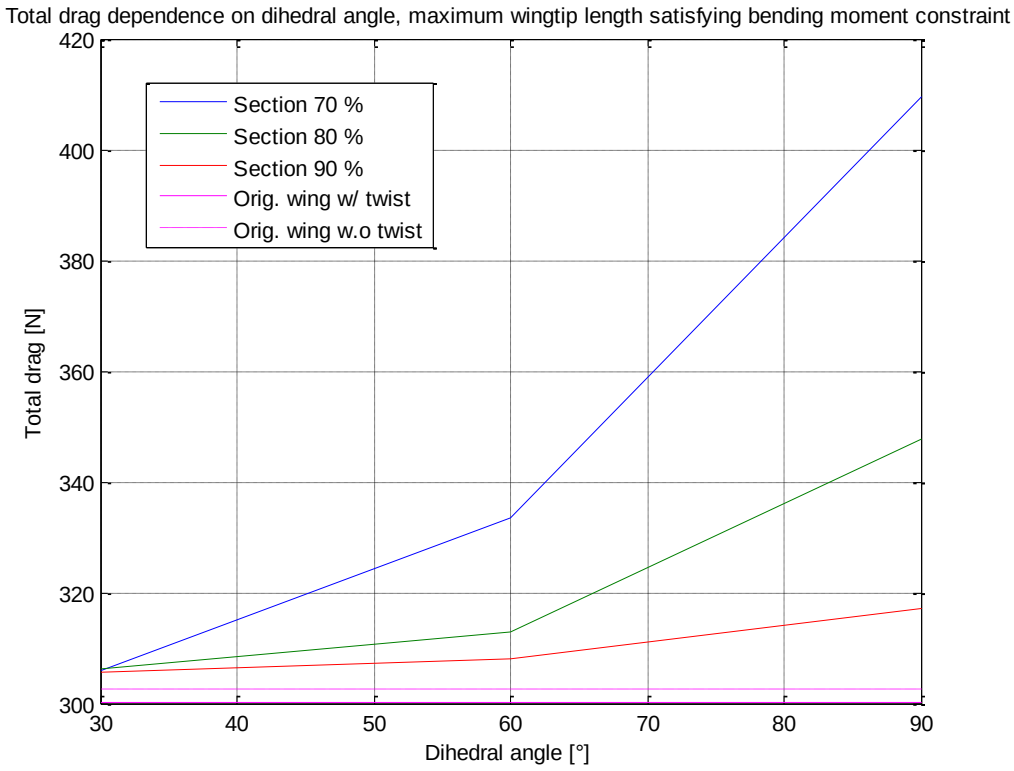

Figure 5.10. Total drag with varying length limited to max. bending moment

6 DISCUSSION AND CONCLUSIONS

6.1 Discussion

The following discussion has been split into three topics to help the reader understand what has been discussed throughout the project. The first topic will take the reader through a time line of how the project has been tackled. Next, the reader will get an in depth explanation on how the results of the project are interpreted. Finally, the reader will get an array of recommendations for alternative tests that may help in future testing of winglets.

6.1.1 Project History

Designing and comparing wings in XFLR5 has not been an easy task. Throughout the project there has arisen several hinders that have taken energy to overcome. From the beginning, learning XFLR5 and all of its functions has been time consuming. There is little information to be found about the program in modern day literature. Most of the learning within the program has been gained from trial and error, as well as reading tips in discussion boards online. Everything from modern winglet design to twist distribution had to be discussed in order to properly execute this project.

From the start, the idea was to design a modified wing for a general aviation aircraft that could easily be applied and would greatly reduce drag. The goal was to reduce the total drag on the wing, while giving it the optimum lift force at a steady level flight. This would in turn minimize fuel consumption, increase flying distance, and reduce air pollution. Here it was decided that a Cessna 172 would be the airplane of choice.

The original thought process was that with the help of winglets on the wing, the above goals could be reached. Here the idea was to design the best winglet possible to apply to a Cessna 172 wing that would reduce drag without affecting the skeleton of the airplane. In turn, this meant that Cessna would have a cheap and easy application to their design that would benefit both the customer and the company economically.

Several problems began to take form after further thought. The main problem being that it is extremely hard to find detailed plans of the entire Cessna 172 as well as it would be difficult to implement in XFLR5. Here, the idea was born to only focus on the wing of the Cessna 172. By shifting the focus to only looking at the wing, the project began to center more on the aerodynamics of the wing instead of the design aspect of building a wing. Attention was now set on studying the effects winglets have on the lift to drag ratios on the airplane wing. A goal was set to modify the Cessna 172 wing to have an optimum lift to drag ratio.

After reading several articles and studying earlier projects involving winglets, it became clear that it would be hard to see any positive effects on the Cessna 172 wing without having to greatly modify the original structure. What felt like an infinite amount of possibilities began to surface; it was now time to limit the wing design in order to fit it into the slotted time limit given for the project. Here the root bending moment constraint was defined for the wing, where this limit may not be passed by more than 0.5%.

Next, it became apparent that the varying wings are harder to compare than originally thought. From the start, most of the focus was set on looking at the lift and drag coefficients, C_L and C_D. It later became clear that only comparing the coefficients was not enough to gain a full understanding if the effects are positive or not. This is mainly due to the wing areas changing as the winglets changed, as seen in Equation (2.16). To solve this, it was decided that XFLR5 was to be analyzed a bit differently. As read earlier in Method, the forces are looked at directly,

instead of studying the coefficients. The mass of the plane was assumed constant, even after winglet changes, this lead to a constant lift that is used for all of the wing modifications.

Lastly, it was determined that it was best to divide the results into looking at induced drag and total drag. The goal officially being that one wants to study a set of different winglets to see their effects on induced drag, as well as seeing the net total effect on drag.

6.1.2 Result Discussion

From the earlier graphs in Results, one can see that most of the predefined tests do not fulfill the requirements for a reduced induced drag for a given constant lift. In Figure 5.4 and Figure 5.5 it looks as if there are three situations where the wings have less induced drag than the original twisted wing. These points are for the wing set-ups:

1. 30° winglet with 80cm length at a 90% section of the wing.
2. 30° winglet with 130cm length at an 80% section of the wing.
3. 30° winglet with 130cm length at a 90% section of the wing.

A closer look at the bending moments at these three points shows that the bending moments at the root chord exceeds the previously defined 1% limit. Therefore, all of the 27 tests seen in Table 4.3 in Method do not accomplish the task of reducing induced drag without surpassing the root bending moment constraint. Upon further examination of the total drag from these varying wingtips that fulfill the bending moment requirements, it can be seen that there is no net benefit to the total drag due to the new wingtips. The total drag increases for all of these modifications.

In Figure 5.6, it can be seen that there are winglet length/angle combinations that do meet the previously set requirements for induced drag. The lengths of the winglets have been maximized for every new winglet angle and position so that the bending moment limit is not passed. Here, the following four combinations result in a Cessna 172 wing with applied winglets that has a reduced induced drag:

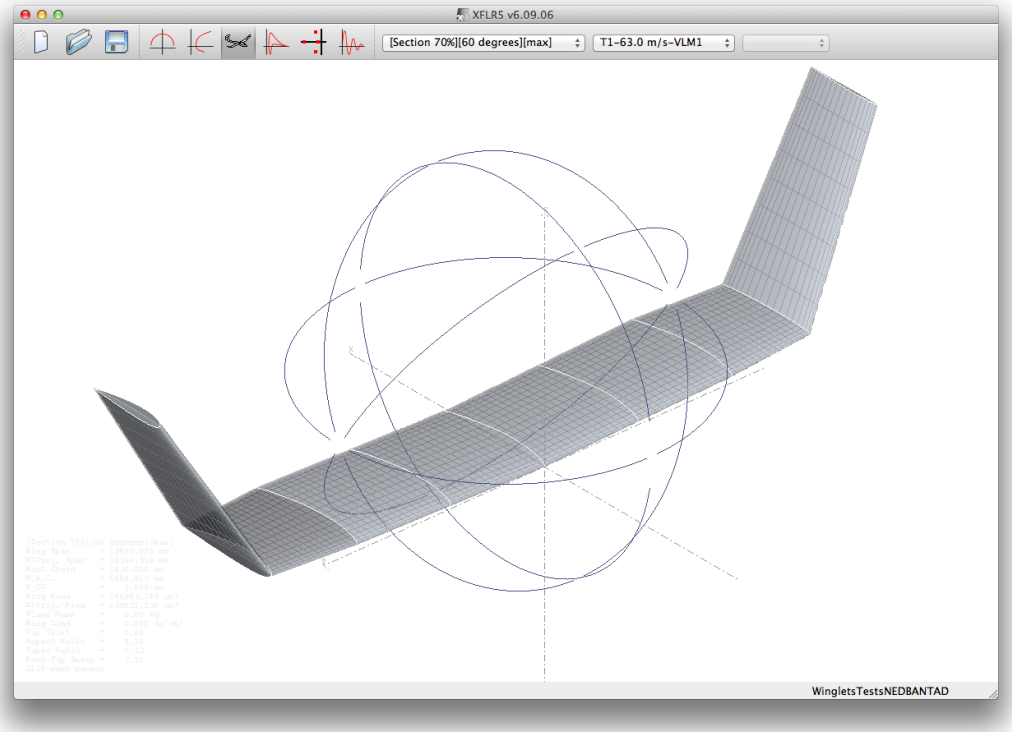

Figure 6.1. 60° winglet with 255cm length at a 70% section of the wing

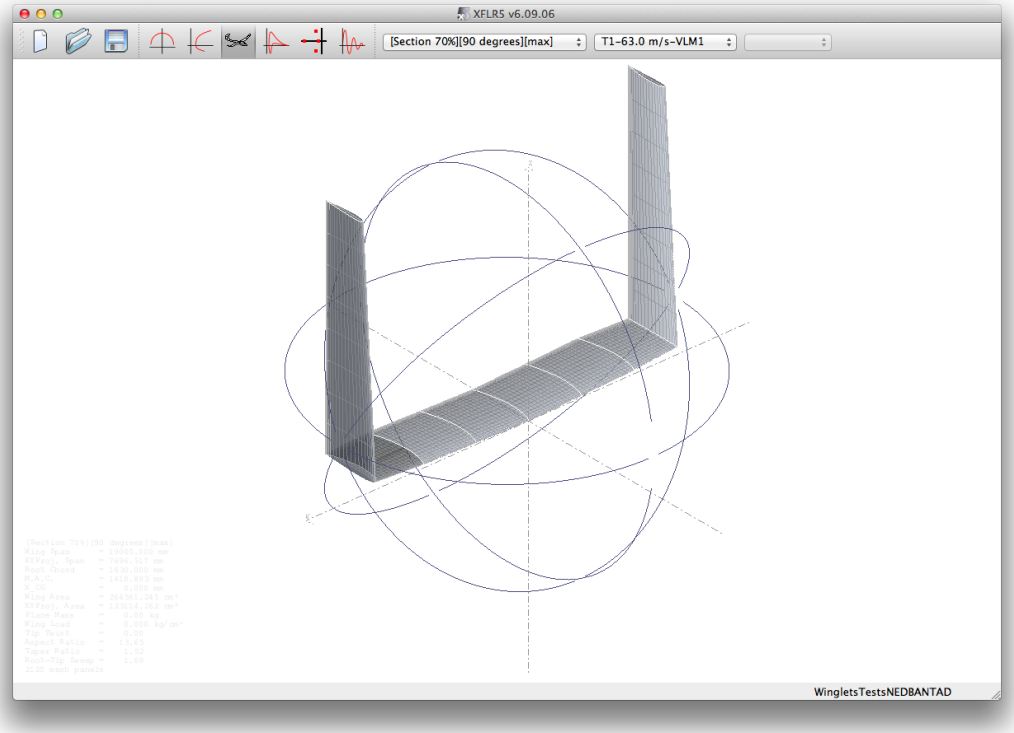

Figure 6.2. 90° winglet with 565cm length at a 70% section of the wing

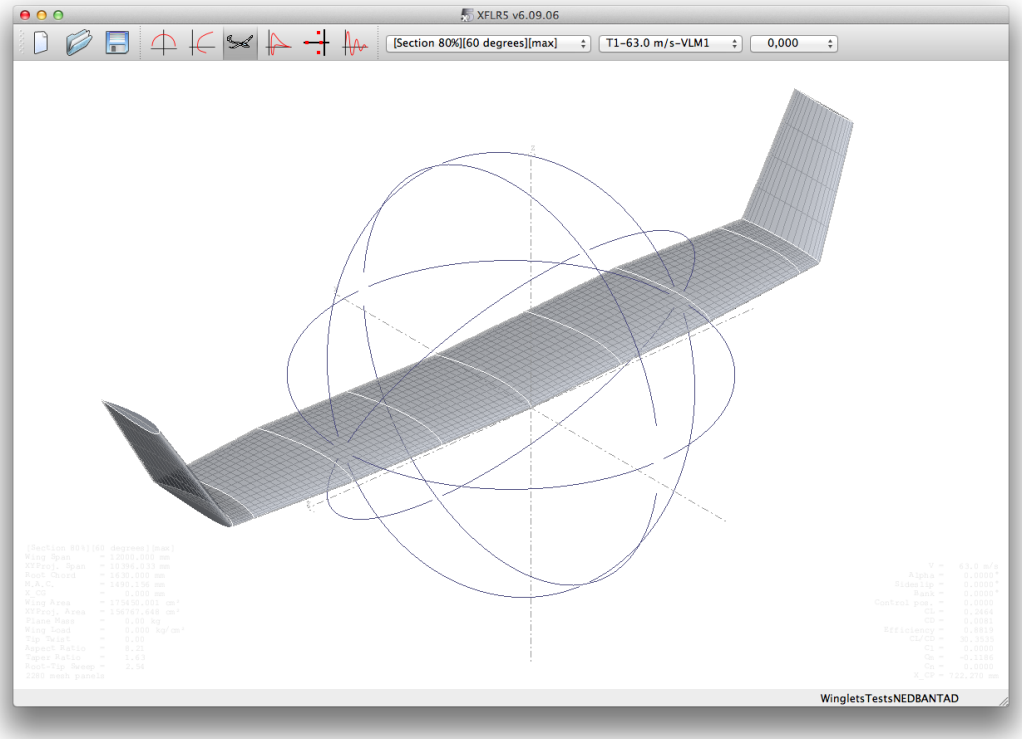

Figure 6.3. 60° winglet with 160cm length at an 80% section of the wing

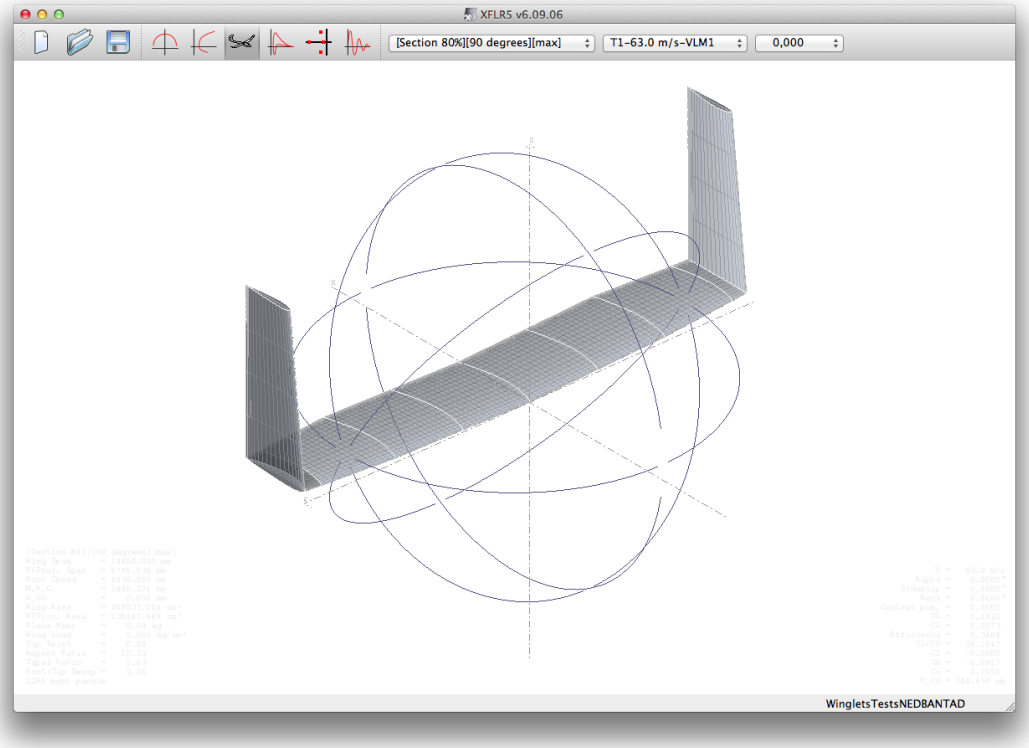

Figure 6.4. 90° winglet with 300cm length at an 80% section of the wing

From the above figures as well as the total drag graphs in Results, it can be seen that these wings are not optimum. The total drag graphs show that although there is a decrease in induced drag, the effects on total drag are still negative. Both the original wing with twist, and the original wing without twist have less total drag than all of the modified maximum winglets. In the above images, one can see that with the exception of Figure 6.3, the winglets look unproportional. When applied to real world situations, these wings would most likely be oversized or too tall for standard general aviation hangars or transports.

Another interesting aspect that can be seen in Figure 5.6 is that it could exist an optimal dihedral angle that minimizes the induced drag for a given root bending moment. This type of winglet design, where the winglet length is increased until the bending moment is maxed, is only valid under the given conditions. As seen in the graph, the induced drag for all three sections look to be at a minimum at 60°. This may be a form of minimum point for varying winglet lengths, although further testing should be done at more dihedral angles to see at which angle winglets have the best effect.

After all of the tests and modifications that could be done within the time given, the best design for a Cessna 172 wing would be the original twisted wing without winglets, that is, the same wing that is currently used. As for induced drag, it is seen that for an increased length in wing or winglet there is a decrease in induced drag. Although, as the wing length increases, the bending moment will increase along the wing. This may result in a restructuring of the wing to compensate for the added bending moment, which in turn most likely will add weight, and decrease the net benefit of the new wing. The above results look to match the earlier Theory chapter. For the tests done in this project, induced drag could be reduced, but the total drag was not beneficial.

6.1.3 Alternative Tests

As discussed above, even if the total drags for the new winglets were not reduced, potential for improvement can still be seen. Although the main goal of the project was to view the effects

winglets have on drag, one may want to use this project as a building block for better winglet design for future aircrafts. One can go back and begin to alter and re-test many of the parameters and variables that have been defined throughout the project. A few recommendations for future testing may include:

- New and better winglet designs
- Increase in bending moment limits
- Varying twist distributions along the wing and winglets
- Different flight conditions
- More detailed winglet junctions

Another interesting aspect would be to design a new wing with winglets already in mind. The project has focused on applying winglets to an already optimized planar wing. Improving the performance of an already effective wing has proved to be challenging. Therefore, it may be easier to design a new wing that has winglets integrated from the beginning. There is more room for adjustment, and the above recommendations can be tested more thoroughly.

6.2 Conclusions

It is no easy task to design and fit a winglet to an existing wing. Extending the wing lengths do result in a decrease in induced drag, although at the expense of increasing the wetted area of the wing. This results in an increase in total drag due to factors such as parasitic drag and inconsistencies in the junction flows. The dihedral angling of the winglets play an important role on the effects of drag as well.

Computation programs such as XFLR5 and MATLAB are worthy tools for wing and winglet testing, although further model testing in wind tunnels or flight tests would be recommended before making complete conclusions. The computational programs offer a quick and easy solution to begin testing, as well as to gain an understanding of the effects that modifications may have on an aircraft.

Careful planning is in order when designing new winglets. Parameters as well as design models need to be discussed and planned in order to get an effective winglet. Good aerodynamic practice is a must to avoid an increase in drag. Changing different parameters will result in varying lift distributions, bending moments, as well as a change in induced drag and total drag. It is important to make just comparisons when looking at different winglets. If not done correctly, the compared data for the winglets is inconclusive.

As seen throughout the project, it is possible to decrease the induced drag on a Cessna 172 wing without surpassing a root bending moment constraint. A good way to make the winglets more effective is to focus on reducing the induced drag while trying to keep the parasitic drag to a minimum.

6.3 Division of Labor

The division of labor has been distributed evenly throughout the project. All three group members have worked together and spent an even amount of time working in XFLR5, MATLAB, and Microsoft Word. Meetings were set up regularly each week, and all of the work was done in computer labs at the KTH campus. All three members are therefore equally responsible for each part of the project process.

7 REFERENCES

[1] http://en.wikipedia.org/wiki/Cessna_172

[2] Jane, Fred T. and Jackson, Paul (eds.). *Jane's All The World's Aircraft*. 100th ed. London: Jane's Information Group. 2013.

[3] McLean, Doug. Wingtip Devices: *What They Do and How They Do It.* Boeing - Aerodynamics, Article 4, 2005.

[4] Milne-Thomson, L. M. *Theoretical Aerodynamics.* Dover Publications, 4th edition, 1958. (PAGE 209)

[5] Karlsson, Arne. *Lifting-line method results for the lateral twist distribution giving an elliptic load distribution.* Dept. of Aeronautical and Vehicle Engineering, KTH. 2014

[6] Karlsson, Arne. *The aeroplane – some basics.* Dept. of Aeronautical and Vehicle Engineering, KTH. 2014

[7] XFLR5 Guidelines, v6.02. 2013. http://sourceforge.net/projects/xflr5/files/, Visited 18 May 2014

[8] Karlsson, Arne. *Steady level flight of an aeroplane with propeller propulsion.* Dept. of Aeronautical and Vehicle Engineering, KTH. 2012

[9] http://www.cessna.com/~/media/Files/Single%20Engine/skyhawk/Skyhawk%202013%20172S%20SD.ashx, Visited 18 May 2014

[10] U.S. Standard Atmosphere. U.S. Government Printing Office. 1976. http://ntrs.nasa.gov/archive/nasa/casi.ntrs.nasa.gov/19770009539.pdf, Visited 18 May 2014

[11] http://www.xflr5.com/docs/Point_Out_Of_Flight_Envelope.pdf, Visited 18 May 2014